Mechanism and kinetics of the atmospheric degradation of perfluoropolymethylisopropyl ether by OH radical: A theoretical study

ARTICLE *in* STRUCTURAL CHEMISTRY · DECEMBER 2014

Impact Factor: 1.84 · DOI: 10.1007/s11224-014-0448-9

3 AUTHORS, INCLUDING:

L. Sandhiya

Ludwig-Maximilians-University of Munich

13 PUBLICATIONS **35** CITATIONS

SEE PROFILE

K. Senthilkumar

Bharathiar University

77 PUBLICATIONS **1,420** CITATIONS

SEE PROFILE

Struct Chem (2014) 25:1773–1783
DOI 10.1007/s11224-014-0448-9

ORIGINAL RESEARCH

Mechanism and kinetics of the atmospheric degradation of perfluoropolymethylisopropyl ether by OH radical: a theoretical study

S. Ponnusamy · L. Sandhiya · K. Senthilkumar

Received: 25 January 2014 / Accepted: 14 May 2014 / Published online: 10 June 2014

Abstract In the present work, the mechanism and kinetics of the reaction of perfluoropolymethylisopropyl ether (PFPMIE) with OH radical are studied. The reaction between PFPMIE and OH radical is initiated through breaking of C–C or C–O bond of PFPMIE. These reactions lead to the formation of COF_2 molecules and alkyl radical. The pathways corresponding to the reaction between PFPMIE and OH radical have been modelled using density functional theory methods M06-2X and MPW1K with 6-31G(d,p) basis set. It is found that the C–C bond breaking reaction is most favourable than the C–O bond breaking reaction. The subsequent reactions of the alkyl radicals, formed from the C–C bond breaking reactions, are studied in detail. The rate constant for the initial oxidation reactions is calculated using canonical variational transition state theory with small curvature tunnelling corrections over the temperature range of 278–350 K. From the calculated reaction, potential energy surface and rate constant, the lifetime and global warming potential of PFPMIE are studied.

Keywords Perfluoropolymethylisopropyl ether · Atmospheric chemical reaction · Global warming potential · Kinetics

Electronic supplementary material The online version of this article (doi:10.1007/s11224-014-0448-9) contains supplementary material, which is available to authorized users.

S. Ponnusamy · L. Sandhiya · K. Senthilkumar (✉)
Department of Physics, Bharathiar University,
Coimbatore 641 046, India
e-mail: ksenthil@buc.edu.in

Introduction

Chlorofluorocarbons (CFCs) and hydrofluorocarbons (HFCs) are used as refrigerants, solvents, fire suppressants and cleaning agent for electronic components [1]. Due to their high stability, these compounds do not degrade easily. Further, the emission of CFCs and HFCs into the atmosphere causes depletion of the ozone layer which results in global warming. In recent years, fluorinated polyethers are found to be the best environmental-friendly alternative for CFCs and HFCs [2–6]. In particular, perfluoropoly ethers (PFPEs) and hydrofluoroethers (HFEs) are used as alternatives for CFCs and HFCs [7–10]. The fluorinated ethers are designed specifically for use in areas of high thermal stress, such as ovens, cookware, industrial and car engines and also in a wide variety of other thermal applications [11]. PFPEs do not contain chlorine atoms, and hence do not contribute to stratospheric ozone depletion, but it may be associated with other environmental effects. For instance, these fluorinated ethers absorb infrared radiation in the 'atmospheric window' ranging between 750 and 1,250/cm [12], which are responsible for global warming. It has been shown in earlier studies that the PFPEs and HFEs have high radiative forcing because of the presence of multiple C–F and C–O bonds [13].

HFEs and PFPEs are known to degrade in the atmosphere through the reaction with OH radical, which is the potent atmospheric oxidizing agent [14]. It is expected that the reaction between perfluoropolymethylisopropyl ether (PFPMIE) and OH radical will proceed in two ways, (i) C–C bond breaking and (ii) C–O bond breaking of PFPMIE by OH radical, yielding COF_2 molecules [15] and alkyl radicals. It is expected that the subsequent reactions of alkyl radical with other atmospheric species will yield substantial amount of other fluorinated species in the atmosphere. The presence of F atoms in the PFPMIE has

increased the global warming potential (GWP) and radiative forcing of PFPMIE. Previous experimental study [7] shows that the atmospheric lifetime of PFPMIE is 800 years, and global warming potential is 1.02 for 20 years time horizon. In the above study, the rate constant was calculated using relative rate technique.

Young et al. [7]. did not study the pathways for the oxidation of PFPMIE by OH radical. To understand the atmospheric oxidation of PFPMIE completely, information about the reaction mechanism and reaction pathways is essential. The contribution of the two reaction channels i.e. C–C bond breaking and C–O bond breaking to the atmospheric degradation of PFPMIE have to be studied in detail. Hence, in the present work, the reaction mechanism and pathways for the degradation of PFPMIE by OH radical in the atmosphere have been studied. The reaction between alkyl radical, a product formed in the primary oxidation reaction, and O_2 has been studied. Peroxy radical formed in the above reaction can react with HO_2 and NO radicals present in the atmosphere. It has been shown that the alkoxy radical formed in the above secondary reactions plays an important role in the degradation mechanism of organic compounds in the atmosphere. The kinetics of the reactions are studied to determine the lifetime and the global warming potential of PFPMIE.

Computational details

In recent studies, the hybrid density functional theory methods, M06-2X [16] and MPW1K [17], have been proved to perform better for the study of reaction mechanism and kinetics [18–20]. Hence, in the present study, the geometry of the minima and first-order saddle points on the potential energy surface of the PEPMIE + OH radical reaction was optimized using M06-2X and MPW1K methods with 6-31G(d,p) basis set. The harmonic vibrational frequency calculations were performed for all the optimized geometries to verify the nature of the stationary points. All minima were confirmed with positive frequencies, and transition state had one imaginary frequency, confirming its location as maxima in one reaction coordinate. The connectivity of transition state structure between designated reactant and product was confirmed for all the studied paths through intrinsic reaction coordinate (IRC) calculations using the second-order algorithm of Gonzalez and Schlegel [21, 22]. The enthalpies of the reaction and Gibb's free energy were calculated by including thermodynamic correction to the potential energy surface at temperature of 298.15 K and 1 atmospheric pressure. All the electronic structure calculations were performed using the Gaussian 09 program package [23].

High pressure limits of thermal rate constant for the initial reactions of PFPMIE with OH radical is calculated using canonical variational transition state theory (CVT) [24–26]. The quantum effect correction for the CVT rate constant was included by small curvature tunnelling (SCT) calculations [27, 28]. The potential energy surface, gradients and hessians obtained from M06-2X/6-31G(d,p) method were directly used to calculate the rate constants. In CVT, high pressure limits of thermal rate constant at temperature T is given by

$$k^{\mathrm{CVT}}(T) = \min_s k^{\mathrm{GT}}(T,s),$$

where

$$k^{\mathrm{GT}}(T,s) = \frac{\sigma k_{\mathrm{B}} T}{h} \frac{Q^{\mathrm{GT}}(T,s)}{\varphi^{\mathrm{R}}(T)} e^{V_{\mathrm{MEP}}(s)/k_{\mathrm{B}}T},$$

where $k^{\mathrm{GT}}(T,s)$ is the generalized transition state theory rate constant at the dividing point s, σ is the symmetry factor accounting for the possibility of more than one symmetry-related reaction path, k_{B} is the Boltzmann constant, h is the Plank's constant, $\varphi^{\mathrm{R}}(T)$ is the reactant partition function per unit volume, $V_{\mathrm{MEP}}(s)$ is the classical potential energy at point s on the minimum energy path, and $Q^{\mathrm{GT}}(T,s)$ is the partition function of a generalized transition state at s. The partition functions for most of the vibrational modes were evaluated by treating them as quantum mechanically separable harmonic oscillators, and the lowest vibrational mode was evaluated by hinder-rotor approximation [29, 30]. The rate constant calculations were performed using the Gaussrate 2009A program [31], which is an interface program between the Gaussian 09 and Polyrate 2010A programs [32].

Results and discussion

The scheme for the reaction between PFPMIE and OH radical is shown in Fig. 1. As shown in Fig. 1, the reaction between PFPMIE and OH radical proceeds either by the breaking of C–C bond or by the breaking of C–O bond of PFPMIE. The PFPMIE decomposes into HF and COF_2 molecules, as observed in the case of the reaction of CF_3-$CFHCF_2OCF_2H$ with OH radical [5]. The C–C bond breaking reaction results in the formation of two COF_2 molecules, and the C–O bond breaking reaction leads to the formation of four COF_2 molecules. The structure of stationary points on the ground-state potential energy surface (PES) of the reaction system optimized at the M06-2X/6-31G(d,p) level of theory is shown in Fig. 2. The relative energy profile of the stationary points on the PES of the PFPMIE + OH reaction is given in Fig. 3. The relative energy (ΔE), enthalpy (ΔH) and Gibb's free energy (ΔG) of the reactive species calculated at M06-2X and MPW1K method with 6-31G(d,p) basis set are summarized in

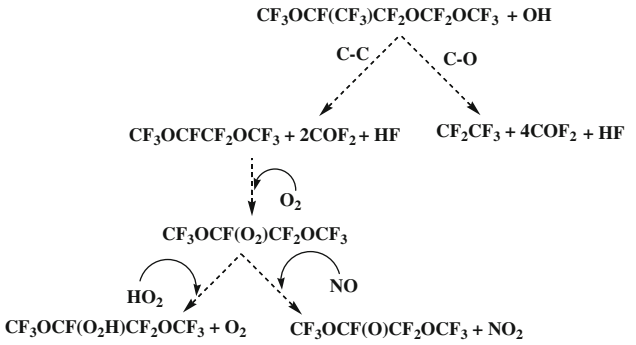

Fig. 1 The reaction scheme for the C–C and C–O bond breaking reactions of PFPMIE by OH radical

Tables 1 and 2. As shown in Tables 1 and 2, the energetics obtained using the two methods are comparable. The average root-mean-square deviation (rmsd) between the internal coordinates obtained from M06-2X and MPW1K methods for the initial C–C bond breaking reaction pathway is 0.01 Å for the reactant, 0.02 Å for the transition state, and 0.02 Å for the intermediate and for the initial C–O bond breaking reaction, the rmsd is 0.02 Å for the reactant, 0.03 Å for the transition state and 0.02 Å for the intermediate. Note that the above-mentioned rmsd values include interactions of both bonded and non-bonded atoms. Hence, the results obtained with M06-2X/6-31G(d,p) level of theory are discussed in detail and are used in further kinetic calculations.

As shown in Fig. 2, the C–C bond breaking reaction is initiated through the breaking of O4–H1 bond of OH radical and C2–C4 bond of PFPMIE (For labelling of atoms, see Fig. 2). The cleaved H-atom binds with the C2-atom of PFPMIE. Thus, the intermediate (I1) is formed through a transition state, TS1 with an energy barrier of 51.44 kcal/mol. In the TS1 structure, the C2–C4 bond is cleaved and the O4-atom of OH radical binds with the C4-atom of PFPMIE. In transition state structure, TS1 the C2–O1 bond distance is 1.992 Å, which was 1.379 Å in the reactant and 1.4 Å in the I1. The C2–C4 bond distance in I1 and TS1 is 3.09 and 2.845 Å, which was 1.581 Å in the reactant. The C2–H1 bond distance is 3.934, 1.082 and 1.121 Å, in the reactant, TS1 and I1, respectively. The significant geometrical deviation of the TS1 from that of the reactant and the calculated energy barrier show that TS1 is a late transition state. The formation of I1 is highly exothermic and exoergic with $\Delta H = -84.13$ kcal/mol and $\Delta G = -81.58$ kcal/mol, respectively.

After the formation of the intermediate, I1, the O4-atom which was eliminated in the first step binds with C2 and H1 atoms, resulting in the formation of an intermediate, I2. This reaction proceeds via transition state, TS2, with an energy barrier of 25.64 kcal/mol. In the transition state structure, the O4 atom binds with C2 atom with a bond length of 1.453 Å and with H1 atom with a bond length of 1.221 Å. The O4–H1 and C2–O4 bond distance of 0.970 and 1.410 Å in TS2 are lower by 2.644 and 2.445 Å from that of I1. Except for this geometrical change, all the other geometrical parameters are similar in I1 and TS2. As given in Table 1, this intermediate formation is exothermic and exoergic by −25.57 and −27.58 kcal/mol, respectively. The intermediate, I2, is converted into another intermediate, I3, in which O1–C2 bond is cleaved and the H1-atom, which was detached from O4 atom abstracts the F1 atom, thereby forming a H1–F1 bond (see Fig. 2). Thus, one COF_2 molecule is eliminated in I3. In this intermediate structure, a halogen bond is existing between H1 and F5 atoms with bond length of 1.952 Å. This multi-step reaction associates with an energy barrier of 21.16 kcal/mol through a transition state, TS3. In the TS3 structure, the O1–C2 bond is cleaved, and H1-atom is placed between O1 and O4 atoms. The O1–C2 bond distance in TS3 has increased by 0.52 Å from that of I2 and H1–F1 bond distance in TS3 is 3.113 Å, which was 4.131 Å in I2. The O1–C2 and H1–F1 bond distance in I3 are 2.609 and 0.927 Å, respectively. This intermediate is formed in a mild exothermic reaction with reaction enthalpy of −2.72 kcal/mol, and the reaction is exoergic with free energy of −10.9 kcal/mol.

The next step in the reaction path is the formation of two COF_2 molecules and $CF_3OCFCF_2OCF_3$ radical and HF molecule (I4). This reaction step is followed through a transition state, TS4, with a small energy barrier of 3.56 kcal/mol. The C2–C3 bond in I3 is cleaved, and F11 atom attached with C5-atom of the radical is abstracted by the C2 atom, and thus a COF_2 molecule is formed. The C2–C3 bond distance is 1.539, 2.298 and 3.790 Å, respectively, in I3, TS4 and I4. Only the C2–C3 bond length variation is observed in TS4, and all the other geometrical parameters are similar in I3 and I4. The formation of the I4 channel is exothermic and exoergic with $\Delta H = -41.96$ kcal/mol and $\Delta G = -31.79$ kcal/mol, respectively.

Another important reaction of PFPMIE with OH radical is C–O bond breaking reaction. The optimized structure of the reactive species is shown in Fig. 4, and relative energy profile of the stationary points on the PES of the C–O bond breaking reaction is given in Fig. 5. The energy barrier (ΔE), enthalpy (ΔH) and Gibbs free energy (ΔG) of the reactive species are summarized in Table 2. The initial C–O bond breaking reaction of PFPMIE by OH radical leads to the formation of an intermediate, I5, in which the σ bond between C4 and O2 atoms of PFPMIE is cleaved. During the formation of intermediate, I5, the O4 atom of OH radical binds with C2 and C4 atoms of PFPMIE. The intermediate, I5, is formed through a transition state, TS5, with an energy barrier of 61.43 kcal/mol. In TS5, the C4–

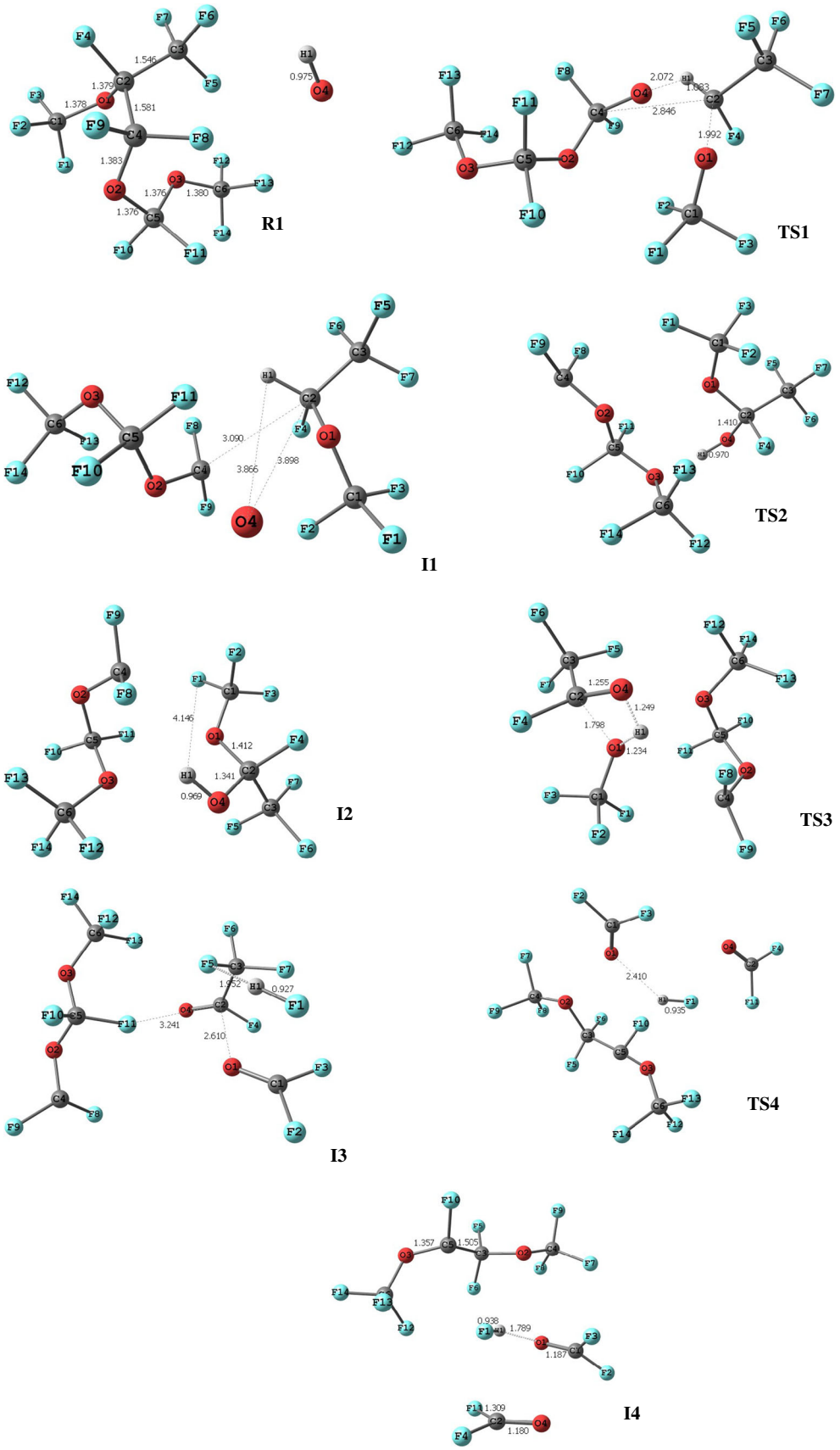

Fig. 2 The optimized structure of the reactive species involved in the C–C bond breaking reacion of PFPMIE by OH radical

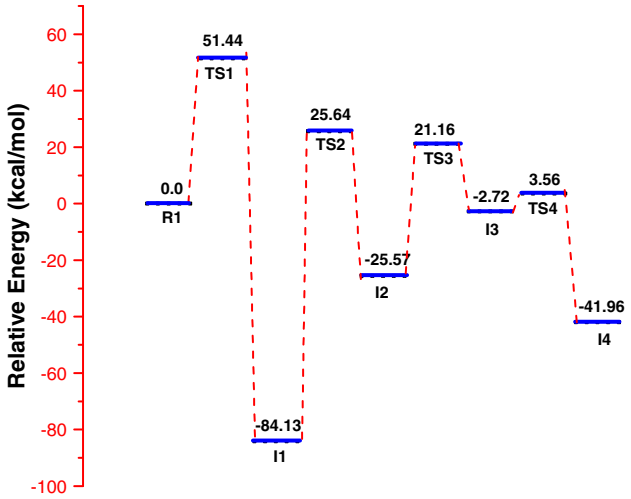

Fig. 3 Relative energy profile of the C–C bond breaking reaction of PFPMIE by OH radical

Table 1 Relative energy (ΔE in kcal/mol), enthalpy of reaction (ΔH in kcal/mol) and Gibb's free energy (ΔG in kcal/mol) of the reactive species involved in the C–C bond breaking reactions of PFPMIE with OH radical calculated at 298 K using M06-2X and MPW1K with 6-31G(d,p) basis set

Species	M06-2X/6-31G(d,p)			MPW1K/6-31G(d,p)		
	ΔE	ΔH	ΔG	ΔE	ΔH	ΔG
R1	0	0	0	0	0	0
TS1	51.44	49.70	48.64	51.39	49.70	48.64
I1	−83.86	−84.13	−81.58	−82.68	−84.13	−81.58
TS2	25.64	24.15	24.16	25.83	24.15	24.16
I2	−27.02	−25.57	−27.58	−26.30	−25.57	−27.58
TS3	21.16	18.68	16.81	20.54	18.12	17.08
I3	−0.69	−2.72	−10.90	−1.54	−2.72	−10.90
TS4	3.56	6.87	8.31	2.32	6.87	8.31
I4	−45.49	−41.96	−31.79	−47.64	−41.96	−31.79

O2 bond distance is 1.30 Å, which is 3.05 Å in the I5. On comparing with reactant, C4–O2 bond distance in I5 was increased by about 1.5 Å. This reaction is endothermic and endoergic with reaction enthalpy of 20 kcal/mol and free energy of 16.16 kcal/mol, respectively. The breaking of C5–O3 bond in I5 leads to the formation of intermediate, I6, through a transition state, TS6, with an energy barrier of 24.54 kcal/mol. In the TS6 structure, the bond between O2 and C6 atoms is cleaved, and F11 atom is abstracted by the H1 atom. In the intermediate, I5, the bond length between C5 and O3-atoms is 1.376 Å and it decreases to 1.26 Å in the intermediate, I6. The formation of I6 is exothermic and exoergic by −24.36 and −20.42 kcal/mol, respectively. The intermediate, I6, is converted into another intermediate, I7, through the breaking of C6–F11 bond. In I7, the

Table 2 Relative energy (ΔE in kcal/mol), enthalpy of reaction (ΔH in kcal/mol) and Gibb's free energy (ΔG in kcal/mol) of the reactive species involved in the C–O bond breaking reactions of PFPMIE with OH radical calculated at 298 K using M06-2X and MPW1K with 6-31G(d,p) basis set

Species	M06-2X/6-31G(d,p)			MPW1K/6-31G(d,p)		
	ΔE	ΔH	ΔG	ΔE	ΔH	ΔG
R2	0	0	0	0	0	0
TS5	61.43	62.12	63.14	61.37	62.40	64.00
I5	21.10	20.00	16.16	19.81	19.00	16.42
TS6	24.54	23.53	21.30	25.32	24.78	22.84
I6	−25.92	−24.36	−20.42	−26.44	−24.02	−22.18
TS7	42.79	40.77	47.89	43.74	41.58	44.24
I7	−52.57	−49.28	−42.87	−48.91	−46.06	−43.92
TS8	23.35	18.69	19.31	22.84	20.26	19.54
I8	−2.67	−4.20	−14.40	−1.44	−3.59	−11.75

hydrogen bond is existing between F11 and H1 atoms with the bond length of 1.90 Å, and H1–F4 bond distance is 0.926 Å. Here, another COF_2 molecule is formed through the transition state, TS7, with an energy barrier of 42.79 kcal/mol. In TS7, the bond length between C6 and F11 atoms is 1.936 Å, which was 1.328 Å in I6. In I7, the F11–H1 bond distance is 1.90 Å, and H1–F4 bond length is 0.926 Å. This intermediate, I7, is formed in an exothermic reaction with ΔH of −49.28 kcal/mol, and the reaction is exoergic with free energy of −42.87 kcal/mol.

The next step in the reaction sequence is the formation of two COF_2 molecules, alkyl radical and HF molecule (I8). This reaction step is followed through a transition state, TS8, with an energy barrier of 23.35 kcal/mol. The C2–O4, C2–C4 and C1–F1 bond in I7 are cleaved, and the F1-atom is attached with C2 atom, and thus four COF_2 molecules are formed. The C2–O4, C2–C4 and C1–F1 bond distances in I7 are 1.42, 1.467 and 1.33 Å and in TS8, and the lengths of those are 3.31, 3.551 and 3.306 Å, respectively. This reaction is exothermic by −4.2 kcal/mol and exoergic by −14.40 kcal/mol. The formation of COF_2 molecules along with alkyl radicals is also observed in the atmospheric degradation of HFEs while reacting with OH radical and Cl-atom [2, 6, 8, 15].

While comparing the energy barrier for the initial C–C and C–O bond breaking reactions, it is observed that the C–C bond breaking reaction is more favourable than the C–O bond breaking reaction. The radicals formed in the atmosphere are prone to undergo reaction with molecular oxygen [33]. Hence, in the present investigation, the reaction between alkyl radical formed in the C–C bond breaking reaction (I4) and O_2 molecule is studied. The optimized structure of the reactive species and relative energy profile involved in the secondary reactions are shown in Figs. S1

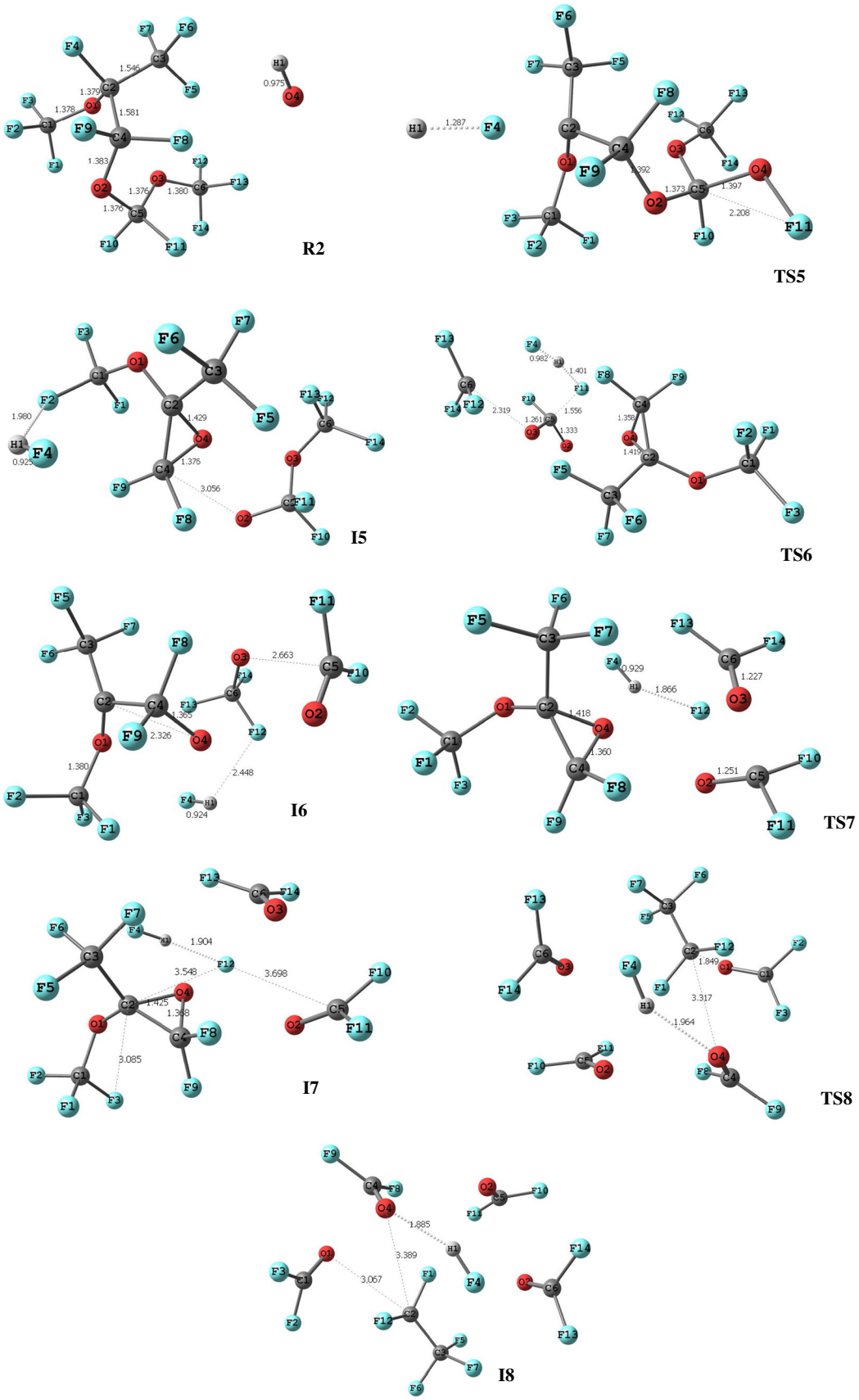

Fig. 4 The optimized structure of the reactive species involved in the C–O bond breaking reaction of PFPMIE by OH radical

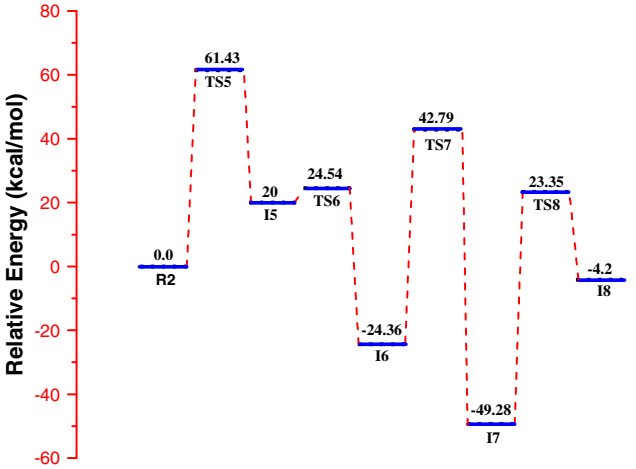

Fig. 5 Relative energy profiles of the C–O bond breaking reaction of PFPMIE by OH radical

and S2. The relative energy (ΔE), enthalpy (ΔH) and Gibb's free energy (ΔG) of the reactive species are summarized in Table 3. As shown in Fig. S2, reaction of alkyl radical, $CF_3OCFCF_2OCF_3$, with O_2 leads to the formation of peroxy radical (I9) in a barrier-less reaction. As shown in Table 2, formation of this intermediate, I9, is exothermic by −32.69 kcal/mol and is exoergic by −28.41 kcal/mol. In the intermediate, I9, the bonding between $CF_3OCFCF_2OCF_3$ and O_2 is relatively weak, and hence the reaction is reversible under tropospheric conditions. In the atmosphere, the peroxy radical (I9) can further react with other radicals. As shown in Fig. S1, the intermediate, I9, can react with HO_2. The terminal O atom of peroxy radical has high electron affinity and abstracts the H-atom from HO_2 and leads to the formation of hydroperoxy adduct, P1 [34, 35]. This reaction occurs through a transition state, TS9, with a small energy barrier of 5.41 kcal/mol. In the product channel, P1, the bond length between O4 and H1 atoms is 0.975 Å, which is 1.8 Å lower than that of the I9 + HO_2. The P1 is formed in an exothermic reaction with reaction enthalpy of −42.79 kcal/mol and is exoergic by −44.92 kcal/mol. At ambient conditions, the peroxy radical, I9, can further react with NO radical present in the atmosphere. In this reaction, the O–O bond of the peroxy radical is cleaved, and NO is oxidized into NO_2. Here, alkoxy radical P2 is formed. This oxidation reaction occurs through the transition state, TS10, with an energy barrier of 11.72 kcal/mol. The P2 is formed in an exothermic reaction with a reaction enthalpy of −21.74 kcal/mol and exoergic by −21.89 kcal/mol.

Kinetics

The kinetics of the initial steps, that is, breaking of C–C and C–O bond, is crucial to determine the fate of PFPMIE in the atmosphere. Hence, the kinetics of the reactions involved in C–C and C–O bond breaking is studied in detail. Since the reactions studied involve tight transition states and the CF3 group rotations are in low frequency modes, the anharmonic effects do not play a significant role in the kinetic analysis [36–38]. Hence, the lack of hindered rotation treatment in the rate calculations does not affect the kinetic results of the studied reactions. Therefore, the kinetics are studied without hindered rotation treatment. From the reaction PES obtained at M06-2X/6-31G(d,p) level of theory, the rate constants were calculated based on canonical variational transition state theory (CVT) with small curvature tunnelling (SCT) corrections. The rate constants calculated using transition state theory (TST), canonical variational transition state theory (CVT), TST with SCT [TST(SCT)] and CVT with SCT [CVT(SCT)] methods for the C–C and C–O bond breaking over the temperature range of 278–350 K are summarized in Tables 4 and 5.

As given in Tables 4 and 5, the rate constant for C–C and C–O bond breaking reactions increases with increase in temperature. The rate constant for C–C reaction at

Table 3 Relative energy (ΔE in kcal/mol), enthalpy of reaction (ΔH in kcal/mol) and Gibb's free energy (ΔG in kcal/mol) of the reaction of $CF_3OCFCF_2OCF_3$ alkyl radical of I4 with O_2 and intermediate, I9 with HO_2 and NO radicals calculated at 298 K using M06-2X/6-31G(d,p) method

Species	ΔE	ΔH	ΔG
$CF_3OCFCF_2OCF_3 + O_2$	0	0	0
I9	−34.94	−32.69	−28.41
I9 + HO_2	0	0	0
TS9	5.41	3.57	3.20
P1	−43.28	−42.79	−44.92
I9 + NO	0	0	0
TS10	11.72	10.93	11.35
P2	−23.06	−21.74	−21.89

Table 4 Rate constant k_{C-C} (in cm^3/molecule/s) of C–C bond breaking reaction of PFPMIE with OH radical

T (k)	TST ($\times 10^{-27}$)	CVT ($\times 10^{-27}$)	TST (SCT) ($\times 10^{-17}$)	CVT (SCT) ($\times 10^{-17}$)
278	0.002	0.002	4.58	4.64
288	0.009	0.009	5.2	5.4
298	0.02	0.02	6.17	6.27
308	0.06	0.08	6.95	6.78
318	0.08	0.24	7.62	7.02
328	0.09	0.63	8.21	7.76
338	1.56	1.55	8.84	8.4
348	3.65	3.63	9.56	9.24
350	4.29	4.27	10.41	10.12

Table 5 Rate constant k_{C-O} (in cm^3/molecule/s) of C–O bond breaking reaction of PFPMIE with OH radical

T (k)	TST ($\times 10^{-31}$)	CVT ($\times 10^{-31}$)	TST(SCT) ($\times 10^{-17}$)	CVT(SCT) ($\times 10^{-17}$)
278	0.0001	0.002	0.001	0.002
288	0.002	0.004	0.04	0.08
298	0.004	0.006	0.52	0.56
308	0.005	0.04	4.1	6.27
318	0.43	0.35	8.64	7.81
328	0.8	0.53	9.51	8.4
338	1.41	1.19	22.23	50.35
348	56.68	4.86	24.62	57.03
350	115.62	99.5	457.21	164.09

298 K using CVT/SCT method is 6.27×10^{-17} cm^3/molecule/s and the rate constant for C–O is 0.56×10^{-17} cm^3/molecule/s. That is, the C–O breaking is slower than the C–C breaking by one order of magnitude. This value is quite comparable with the experimental value of 6.8×10^{-16} cm^3/molecule/s [7]. From Tables 4 and 5, it is observed that the ratio between CVT and TST rate constant is 1 over the whole temperature range studied except at temperatures 318 and 328 K. At temperatures 318 and 328 K, the variational effect is 3 and 7, respectively. At temperatures 318 and 328 K, the variational transition state is located at $s = 0.05$ Å away from the reference position. Hence, the variational effect is appreciable at these temperatures. This type of behaviour has been previously observed in various atmospheric reactions [39–42]. The ratio between CVT with SCT rate constant and CVT rate constant, and also ratio between TST with SCT rate constant to TST rate constant for C–C and C–O reactions show that the tunnelling effect on the reaction rate constant is appreciable and is in the order of 10^{10}.

The vibrationally adiabatic ground-state potential energy (V_a^G) and the classical potential energy (V_C) curves as a function of reaction coordinate for both C–C and C–O reactions are shown in Figs. 6 and 7. Figures 6 and 7 show that the C–C and C–O have similar adiabatic ground-state potential energy (V_a^G) curves, whereas the maximum of V_C curve appear at 48 and 65 kcal/mol for C–C and C–O reactions. The Arrhenius plot for C–C and C–O bond breaking reaction is shown in Fig. 8. The Arrhenius activation energies at 298 K for the C–C and C–O are 1.10 and 14.2 kcal/mol, respectively. That is, the PFPMIE will dissociate into reaction products through C–C. The temperature dependence of the rate constant calculated for the two reactions shows that the oxidative degradation of PFPMIE occurs rapidly in the lower layer of the troposphere. The calculated branching ratio for C–C and C–O bond breaking is shown in Fig. 9(a, b). The plot shows that at 298 K, the

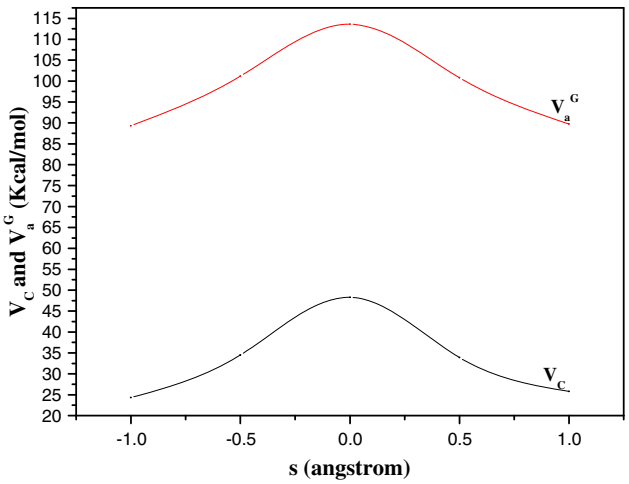

Fig. 6 Calculated V_C and V_a^G versus reaction coordinate S for the C–C bond breaking reaction of PFPMIE with OH radical

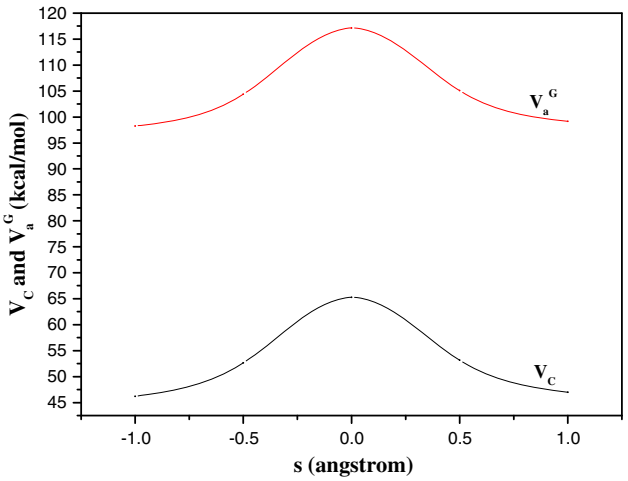

Fig. 7 Calculated V_C and V_a^G versus reaction coordinate S for the C–O bond breaking reaction of PFPMIE with OH radical

contribution of C–C bond breaking reaction is larger than that of the C–O to the atmospheric degradation of PFPMIE by OH radical.

On comparing the energetics and kinetics of the initial C–C and C–O bond breaking reactions, it is observed that the C–C is kinetically and thermodynamically favourable than the C–O. Hence, the lifetime and global warming potential of PFPMIE are calculated based on the rate constant calculated for C–C bond breaking reaction.

Atmospheric lifetime and global warming potential

The atmospheric lifetime, (τ), of PFPMIE is estimated from the rate constant calculated for the reaction of

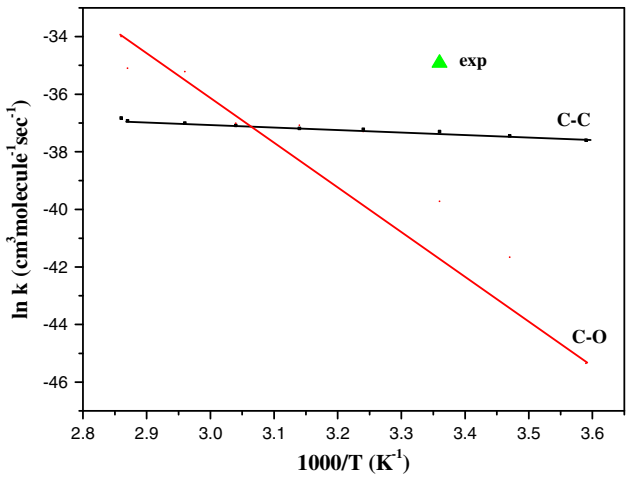

Fig. 8 Arrhenius plot of the rate constant corresponding to C–C and C–O bond breaking reactions

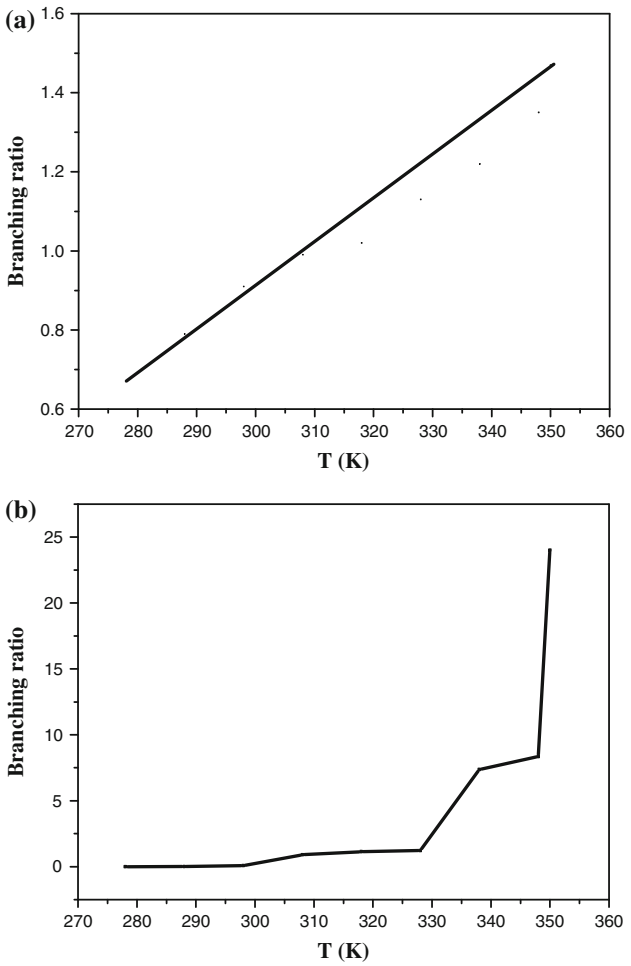

Fig. 9 The branching ratio of the C–C and C–O bond breaking reaction of PFPMIE with OH radical

PFPMIE with OH radical. The atmospheric lifetime is calculated using the relation

$$\tau = \frac{1}{k_{OH}[OH]},$$

where k_{OH} is the rate constant of C–C and the concentration of OH radical and [OH] in the atmosphere is 9.4×10^5 radicals/cm [43]. Using this expression, the lifetime of PFPMIE is calculated as 519 years. The lifetime of PFPMIE calculated from experimental methods is 800 years [7]. The difference between the theory and experimental results is due to the fact that, in the study of Young et al. [7], the lifetime is calculated for the oxidation of PFPMIE into alky radical and COF_2 molecules, whereas in the present study, the lifetime is calculated using the rate constant calculated for the initial C–C bond breaking reaction alone.

Using the calculated lifetime and the information obtained from the infrared absorption spectra of the transition state, TS1, the GWP of PFPMIE is calculated. The IR intensity and the force corresponding to the reactive vibrational mode in the TS1 structure are used to calculate the radiative forcing (a_i) [44–47]. From the calculated a_i and τ, the GWP of PFPMIE is calculated relative to the absolute global warming potential (AGWP) of CFC-11 for 20 years time horizon (t). In terms of a_i and τGWP is given by

$$\mathrm{GWP} = \frac{a_i \int_0^t e^{\frac{-t}{\tau}} d\tau}{\mathrm{AGWP}_{\mathrm{CFC}-11}}.$$

The AGWP of CFC_{11} is 6,300 years relative to CO_2 for 20 years time horizons [48]. The calculated GWP of PFPMIE for 20 years time horizon is 1.40 relative to CFC_{11}. This value is comparable with the experimentally calculated GWP of 1.02 for PEPMIE relative to CFC_{11} for 20 years time horizon [7]. The atmospheric degradation of PFPMIE leads to the formation of fluorinated radical species as observed for degradation of HFCs and HFEs, and hence the use of PFPMIE does not deplete the stratospheric ozone, since it does not contain Cl atoms.

Conclusions

In the present work, the atmospheric degradation of Perfluoropolymethylisopropyl ether (PFPMIE) through oxidation reaction with OH radical is studied using density functional theory and canonical variational transition state theory. From the analysis of the results, the following main conclusions are arrived:

1. The reaction between PFPMIE and OH radical is initiated through the breaking of C–C and C–O bond of

PFPMIE. The calculated energy barrier show that the C–C bond breaking reaction is kinetically favourable than the C–O bond breaking reaction.

2. The rate constants calculated for the C–C and C–O bond breaking reactions are 6.27×10^{-17} and 0.56×10^{-17} cm^3/molecule/s, respectively.
3. The calculated lifetime of PFPMIE is 519 years, which suggests a large global warming potential. For a 20 year time horizon, the global warming potential of PFPMIE is 1.40 relative to CFC_{11} which is in good agreement with the experimental results for similar compounds [7]. The results obtained from the present investigation confirm that the PFPMIE is the best alternative for CFCs.

Acknowledgments The authors thank the University Grants Commission (UGC), Govt. of India, for granting the Major Research Project. The authors thank the reviewer for giving valuable suggestions to improve the manuscript.

References

1. EPA US. Environmental protection Agency Clean Air Act. http://www.epa.gov/ozone/snap/index.html
2. Bravo I, Diaz-de-Mera Y, Aranda A, smith k (2010) Atmospheric chemistry of $C_4F_9OC_2H_5$ (HFE-7200), $C_4F_9OCH_3$ (HFE-7100), $C_3F_7OCH_3$ (HFE-7000) and $C_3F_7CH_2OH$: temperature dependence of the kinetics of their reactions with OH radicals, atmospheric lifetimes and global warming potentials. Phys Chem Chem Phys 12:5115–5125
3. Oyaro N, Sellevag SR, Nielsen OJ (2004) Study of the OH and Cl-initiated oxidation, IR absorption cross-section, radiative forcing, and global warming potential of four C_4-hydrofluoroethers. Environ Sci Tech 38:5567–5576
4. Sulbaek Andersen MP, NIelsen OJ, Wallington TJ, Hurley MD, DeMore WB (2005) Atmospheric chemistry of $CF_3OCF_2CF_2H$ and $CF_3OC(CF_3)_2H$: reaction with Cl atoms and OH radicals, degradation mechanism, global warming potentials, and empirical relationship between k(OH) and k(Cl) for organic compounds. J Phys Chem A 109:3926–3934
5. Wallington TJ, Hurley MD (2004) Atmospheric chemistry of $CF_3CFHCF_2OCF_3$ and $CF_3CFHCF_2OCF_2H$: reaction with Cl atoms and OH radicals, degradation mechanism, and global warming potentials. J Phys Chem A 108:11333–11338
6. Christensen LK, Sehested J, NIelsen OJ, Bilde M, Wallington TJ, Guschin A, Molina LT, Molina MJ (1998) Atmospheric chemistry of HFE-7200 ($C_4F_9OC_2H_5$): reaction with OH radicals and fate of $C_4F_9OCH_2CH_2O(\bullet)$ and $C_4F_9OCHO(\bullet)CH_3$ radicals. J Phys Chem A 102:4839–4845
7. Young CJ, Hurley MD, Wallington TJ, Mabury SA (2006) Atmospheric lifetime and global warming potential of a perfluoropolyether. Environ Sci Tech 40:2242–2246
8. Garzon A, Antinolo M, Moral M, Notario A, Jimenez E, Gomez MF, Albaladejo J (2013) An experimental and theoretical study on the reaction of Cl with $CF_3CF_2CH_2OH$. Mol Phys 111(6):753–763
9. Chakrabartty AK, Mishra BK, Bhattacharjee D, DR C (2013) Mechanistic and kinetics study of the gas phase reactions of methyltrifluoroacetate with OH radical and Cl atom. Mol Phys 111(7):860–867
10. Singh HJ, Gour NK, Srivastava P (2013) Computational studies on the thermal decomposition of the $CH_2FOCHFO$ radical. Mol Phys. doi:10.1080/00268976.2013.785612
11. Ellis DA, Mabury SA, Martin JW, Derek CGM (2001) Thermolysis of fluoropolymers as a potential source of halogenated organic acids in the environment. Nature 412:321–324
12. Bravo I, Aranda A, Hurley MD, Marston G, Nutt DR, Shine KP (2010) Infrared absorption spectra, radiative efficiencies, and global warming potentials of perfluoro carbons: comparison between experiment and theory. J Geophys Res 115:D24317
13. Bravo I, Diaz-de-Mera Y, Aranda A, Moreno E, Nutt DR, Marston G (2011) Radiative efficiencies for fluorinated esters: indirect global warming potentials of hydrofluoroethers. Phys Chem Chem Phys 13:17185
14. Thompson AM (1992) The oxidizing capacity of the earth's atmosphere: probable past and future changes. Science 256:1157
15. Wallington TJ, Schneider WF, Sehested J, Bilde M, Platz J, Nielsen OJ, Christensen LK, Molina MJ, Molina LT, Wooldridge PW (1997) Atmospheric chemistry of HFE-7100 ($C_4F_9OCH_3$): reaction with OH radicals, UV spectra and kinetic data for $C_4F_9OCH_2$ and $C_4F_9OCH_2O_2$ radicals, and the atmospheric fate of $C_4F_9OCH_2O$ radicals. J Phys Chem A 101:8264–8274
16. Zhao Y, Truhlar DG (2008) The M06 suite of density functionals for main group thermochemistry, thermochemical kinetics, noncovalent interactions, excited states, and transition elements: two new functionals and systematic testing of four M06-class functionals and 12 other functionals. Theor Chem Acc 120(1–3):215–241
17. Lynch BJ, Fast PL, Harris M, Truhlar DG (2000) Adiabatic connection for kinetics. J Phys Chem A 104:4811
18. Karton A, Tarnopolsky A, Lamere JF, Schatz G, Martin JML (2008) Highly accurate first-principles benchmark data sets for the parametrization and validation of density functional and other approximate methods. Derivation of a robust, generally applicable, double-hybrid functional for thermochemistry and thermochemical kinetics. J Phys Chem A 112:12868
19. Li. Q. S, Xu. X. D, S. Z (2004) Predicting energies and geometries for reactions involved in atmosphere chemistry: a comparison study between hybrid DFT methods. Chem Phys Lett 384:20
20. Zheng G, Zhao Y, Truhlar DG (2007) Thermochemical kinetics of hydrogen-atom transfers between methyl, methane, ethynyl, ethyne, and hydrogen. J Phys Chem A 111:4632
21. Gonzalez C, Schlegel HB (1989) An improved algorithm for reaction path following. J Chem Phys 90:2154–2161
22. Gonzalez C, Schlegel HB (1990) Reaction path following in mass weighted internal coordinates. J Chem Phys 94:5523–5527
23. Frisch MJ, Trucks GW, Schlegel HB, Scuseria GE, Robb MA, Cheeseman JR, Scalmani G, Barone V, Mennucci B, Petersson GA, Nakatsuji H, Caricato M, Li X, Hratchian HP, Izmaylov AF, Bloino J, Zheng G, Sonnenberg JL, Hada M, Ehara M, Toyota K, Fukuda R, Hasegawa J, Ishida M, Nakajima T, Honda Y, Kitao O, Nakai H, Vreven T, Montgomery JA, Jr., Peralta JE, Ogliaro F, Bearpark M, Heyd JJ, Brothers E, Kudin KN, Staroverov VN, Kobayashi R, Normand J, Raghavachari K, Rendell A, Burant JC, Iyengar SS, Tomasi J, Cossi M, Rega N, Millam JM, Klene M, Knox JE, Cross JB, Bakken V, Adamo C, Jaramillo J, Gomperts R, Stratmann RE, Yazyev O, Austin AJ, Cammi R, Pomelli C, Ochterski JW, Martin RL, Morokuma K, Zakrzewski VG, Voth GA, Salvador P, Dannenberg JJ, Dapprich S, Daniels AD, Farkas O, Foresman JB, Ortiz JV, Cioslowski J, Fox DJ (2009). Gaussian 09, Revision B01, Gaussian, Inc Wallingford CT
24. Garrett BC, Truhlar DG (1979) Generalized transition state theory. Bond energy-bond order method for canonical variational calculations with application to hydrogen atom transfer reactions. J Am Chem Soc 101(16):4534

25. Garrett BC, Truhlar DG (1979) Criterion of minimum state density in the transition state theory of bimolecular reactions. J Chem Phys 70:1593
26. Garrett BC, Truhlar DG, Grev RS, Magnuson AW (1980) Improved treatment of threshold contributions in variational transition-state theory. J Phys Chem 84(13):1730–1748
27. Liu YP, Lynch GC, Truong TN, Lu DH, Truhlar DG, Garrett BC (1993) Molecular modeling of the kinetic isotope effect for the [1,5]-sigmatropic rearrangement of cis-1,3-pentadiene. J Am Chem Soc 115(6):2408
28. Lu DH, Truong TN, Melissas VS, Lynch GC, Liu YP, Garrett BC, Steckler R, Issacson AD, Rai SN, Hancock GC, Lauderdale JG, Joseph T, Truhlar DG (1992) POLYRATE 4: a new version of a computer program for the calculation of chemical reaction rates for polyatomics. Comput Phys Commun 71(3):235
29. Chaung YY, Truhlar DG (2000) Statistical thermodynamics of bond torsional modes. J Chem Phys 112:1221
30. Truhlar DG (1991) A simple approximation for the vibrational partition function of a hindered internal rotation. J Comput Chem 12(2):266
31. Zheng J, Zhang S, Corchado JC, Chuang YY, Coitino EL, Ellingson BA, Truhlar DG (2009) GAUSSRATE, version 2009. University of Minnesota, Minneapolis
32. Zheng J, Zhang S, Corchado JC, Chaung YY, Fast PL, Hu WP, Liu YP, Lynch GC, Nguyen KA, Jackels CF, Ramos AF, Ellingson BA, Melissas VS, Villa J, Rossi I, Coitino EL, Pu J, Albu TV (2010) POLYRATE, version 2010. University of Minnesota, Minneapolis
33. Atkinson K, Arey J (2003) Atmospheric degradation of volatile organic compounds. J Chem Rev 103:4605
34. Singh HJ, Mishra BK (2010) Ab initio studies on the reactivity of the CF_3OCH_2O radical: thermal decomposition versus reaction with O_2. J Mol Model 16:1473
35. Christensen LK, Wallington TJ, Guschin A, Hurley MD (1999) Atmospheric degradation mechanism of CF_3OCH_3. J Phys Chem A 103:4202
36. Lavado EG, Corchado JC, Suleimanov YV, Green WH, Joaquin EJ (2014) Theoretical kinetic study of the $O(^3P)$ $+CH_4/CD_4$ hydrogen abstraction reaction: the role of anharmonicity, recrossing effects and quantum mechanical tunneling. J Phys Chem A. doi:10.1021/jp5028965
37. Ramos AF, Miller JA, Klippenstein SJ, Truhlar DG (2006) Modeling the kinetics of bimolecular reactions. Chem Rev 106:4518–4584
38. Truhlar DG, Garrett BC, Klippenstein SJ (1996) Current status of transition-state theory. J Phys Chem 100:12771–12800
39. Chow R, Ng M, Mok DKW, Lee EPF, Dyke JM (2014) Rate coefficients of the $Cl + CH_3C(O)OCH_3 \rightarrow HCl + CH_3C(O)OCH_2$ reaction at different temperatures calculated by transition-state theory with ab initio and density functional theory reaction paths. J Phys Chem A 118:2040–2055
40. Li QS, Yang J, Zhang S (2006) Reaction-path dynamics and theoretical rate constants for the CHnF4-*n* + O3 f HOOO + CH*n*-1F4-*n* (*n*) 2,3) reactions. J Phys Chem A 110:11113–11119
41. Zhang Q, Wang S, Zhou J, Y G (2002) Ab initio and kinetic calculation for the abstraction reaction of atomic O(3*P*) with SiH_4. J Phys Chem A 106:115–121
42. Galano A, Cruz-Torres A, A-I R (2006) Isopropylcyclopropane +OH gas phase reaction: a quantum chemistry +CVT/SCT approach. J Phys Chem A 110:1917–1924
43. Prinn RG, Huang J, Weiss RF, Cunnold DM, Fraser PJ, Simmonds PG, McCulloch A, Harth C, Salameh P, O'Doherty S, Wang RHJ, Porter L, Miller BR (2001) Evidence for substantial variations of atmospheric hydroxyl radicals in the past two decades. Science (Washington, DC, US) 292:1882–1887
44. Naik V, Jain AK, Patten KO, Wuebbles DJ (2000) Consistent sets of atmospheric lifetimes and radiative forcings on climate for CFC replacements: hCFCs and HFCs. J Geophys Res 105: 6903–6914
45. Papasavva S, Tai S, Illinger KH, Kenny JE (1997) Infrared radiative forcing of CFC substitutes and their atmospheric reaction products. J Geophys Res 102:13643–13650
46. Grossman AS, Grant KE (1997) Radiative forcing calculations for CH_3Cl and CH_3Br. J Geophys Res 102:13651–13656
47. Pinnock S, Hurley MD, Shine KP, Wallington TJ, Smyth TJ (1995) Radiative forcing of climate by hydrochlorofluorocarbons and hydrofluorocarbons. J Geophys Res 100:23227–23238
48. Orkin VL, Villenave E, Huie RE, Kurylo MJ (1999) Atmospheric lifetimes and global warming potentials of hydrofluoroethers: reactivity toward OH, UV spectra, and IR absorption cross sections. J Phys Chem A 103:9770–9779